Accepted Manuscript

Title: Electrodeposited Nitrogen-Doped Graphene/Carbon Nanotubes Nanocomposite as Enhancer for Simultaneous and Sensitive Voltammetric Determination of Caffeine and Vanillin

Author: Lin Jiang Yaping Ding Feng Jiang Li Li Fan Mo

PII: S0003-2670(14)00582-0
DOI: http://dx.doi.org/doi:10.1016/j.aca.2014.05.010
Reference: ACA 233254

To appear in: *Analytica Chimica Acta*

Received date: 6-2-2014
Revised date: 2-5-2014
Accepted date: 6-5-2014

Please cite this article as: Lin Jiang, Yaping Ding, Feng Jiang, Li Li, Fan Mo, Electrodeposited Nitrogen-Doped Graphene/Carbon Nanotubes Nanocomposite as Enhancer for Simultaneous and Sensitive Voltammetric Determination of Caffeine and Vanillin, Analytica Chimica Acta http://dx.doi.org/10.1016/j.aca.2014.05.010

Electrodeposited Nitrogen-Doped Graphene/Carbon Nanotubes Nanocomposite as Enhancer for Simultaneous and Sensitive Voltammetric Determination of Caffeine and Vanillin

Lin Jiang, Yaping Ding*, Feng Jiang, Li Li, Fan Mo

Department of Chemistry, Shanghai University, Shanghai 200444, P. R. China.

*Corresponding author. E-mail: wdingyp@sina.com; Fax: +86 21 66132797; Tel: +86 21 66134734

Graphical abstract

A nanocomposite of nitrogen-doped graphene (NGR) and nitrogen-doped carbon nanotubes (NCNTs) was first modified onto an electrode through electrodeposition method and employed to sensitively detect caffeine and vanillin simultaneously for the first time.

Highlights

- The first electrochemical sensor for caffeine (CAF) and vanillin (VAN).
- NGR-NCNTs was modified through electrodeposition for the first time.
- The sensor was qualified for real sample determination with satisfactory results.

Abstract

A nitrogen-doped graphene/carbon nanotubes (NGR-NCNTs) nanocomposite was employed into the study of the electrochemical sensor via electrodeposition for the first time. The morphology and structure of NGR-NCNTs nanocomposite were investigated by scanning electron microscopy (SEM) and transmission electron microscopy (TEM),

respectively. Meanwhile, the electrochemical performance of the glassy carbon electrode (GCE) modified with electrodeposited NGR-NCNTs (ENGR-NCNTs/GCE) towards caffeine (CAF) and vanillin (VAN) determination was demonstrated by cyclic voltammetry (CV) and square wave voltammetry (SWV). Under optimal condition, ENGR-NCNTs/GCE exhibited a wide linearity of 0.06-50 μM for CAF and 0.01-10 μM for VAN with detection limits of 0.02 μM and 3.3×10^{-3} μM, respectively. Furthermore, the application of the proposed sensor in food products was proven to be practical and reliable. The desirable results show that ENGR-NCNTs nanocomposite has promising potential in electrocatalytic biosensor application.

Keywords: Nitrogen-doped graphene/carbon nanotubes; Electrodeposition; Ultrasensitive; Electrochemical sensor

1. Introduction

Chemical-doping method represents a powerful tool for modifying the electronic and chemical properties of the host materials. It has already played a vital role in the research of material chemistry and electrochemistry. [1-5] In the last few years, nitrogen acting as the dopant of carbon-based materials has attracted considerable attention [6-13] because of its comparable atomic size and five valance electrons to form strong valence bonds with carbon atoms [14]. Meanwhile, as to the nitrogen-doped (N-doped) host material, graphene (GR) and carbon nanotubes (CNTs)

also have been extensively studied as both of them exhibit excellent electrochemical performance in the field of biosensors [15-16], lithium batteries [17-18], and supercapacitors [19-20]. On the basis of the excellent combination of nitrogen atom with GR and CNTs, N-doped GR (NGR) and N-doped NCNTs (NCNTs) are widely reported to have played a more active role in energy storage [21], oxygen reduction [23,24-25], electrochemiluminescence [26] and biosensors [22,27-39] over their undoped counterparts. For example, Zhang et al. [24] synthesized a 3D NCNTs based on the mechanical support of GR sheets and the as-prepared NCNTs/GR composite, which manifested a high electrocatalytic activity for the oxygen reduction reaction (ORR). Wu et al. [27] reported a CuO/N-reduction graphene oxide (N-rGO) nanocomposite that had a much higher ORR activity than CuO/GO and N-rGO. Besides that, a NGR obtained from thermal annealing of graphite and melamine showed excellent electrocatalytic activity towards the oxidation of ascorbic acid, dopamine and uric acid. [29] All these applications prove that NGR and NCNTs can be the promising enhancers of both catalytic activity and sensitivity in electrochemical sensors.

Caffeine (1, 3, 7-trimethylxanthine) (CAF) and vanillin (VAN) are two common additives and often coexist in many snacks and beverage products. As is well known, CAF is a xanthine alkaloid and nature stimulant that can effectively hype the central nervous system of advanced living organisms. Owing to its distinct flavor and powerful psychoactive effect, CAF has long been an irreplaceable part in the food and drink

systems. Meanwhile, vanillin (VAN) has been acting as an indispensable smell additive in most of the desserts and beverages (like chocolate, cookies and many other food and drink products), which attract a large number of customers, especially the young. However, overtaking of CAF and VAN can lead to some undesirable consequences to their consumers. Specifically, high-dose of CAF can cause severe side effects, including oversensitivity, irritability, anxiety, insomnia, etc., which gravely threaten people's health and hence lower their life quality in the long run. Besides, excessive ingestion of VAN can also cause potential damage to human liver and kidney. Worse still, the addiction of food or drinks containing CAF and VAN is highly likely to induce a vicious circle since CAF has severe addictive effect and the seductive smell of VAN may entice a constant appetite. Therefore, from the viewpoint of food safety and addiction prevention, simultaneous determination of CAF and VAN in food products is of vital significance and necessity for people, especially for growing children. Till now, although there have been plenty of reports about the electrochemical sensors of CAF [40-43] or VAN [44-45] respectively, the simultaneous determination of CAF and VAN have been rarely released.

Herein, we report the first electrochemical sensor of CAF and VAN based on electrodeposited NGR-NCNTs nanocomposite (ENGR-NCNTs) as the electrochemical enhancer. To the best of our knowledge, this is the first attempt for N-doped carbon materials to modify the electrode through electrochemical modification method. In this work, the NGR-NCNTs nanocomposite was electrodeposited onto the glassy carbon

electrode (GCE) through potentiostatic method from the KCl aqueous solution containing homogeneous NGR-NCNTs. The obtained ENGR-NCNTs showed remarkable electrocatalysis response to CAF and VAN oxidation. This can be attributed to the excellent conductivity and effective catalytic ability of NGR and NCNTs. Furthermore, the GCE modified with ENGR-NCNTs (ENGR-NCNTs/GCE) was applied into the food sample determination with satisfactory recoveries. Promisingly, the NGR-NCNTs can be an employable candidate in the platform of electrochemical sensor.

2. Experimental

2.1 Reagents and apparatus

NGR-NCNT was synthesized according to a reported hydrothermal route. [46] CAF, VAN, alanine, phenylalanine, leucine, cysteine, uric acid, ascorbic acid and citric acid were purchased from Aladdin Chemical Reagent Co., Ltd. (Shanghai, China). Glucose, maltose, sucrose and other chemicals were obtained from Sinopharm Chemical Reagent Co., Ltd. (SCRC, China). All chemicals employed in this work were analytical grade. All experiments were performed in 0.01 M sulfuric acid solution (0.01 M H_2SO_4) and double distilled water (DDW) was used throughout. The real samples of CAF and VAN were purchased from the local department store. All electrochemical experiments were carried out at room temperature.

Electrochemical experiments including cyclic voltammetry (CV), square wave voltammetry (SWV) and electrochemical impedance spectroscopy (EIS) were all

carried out with a CHI 660D electrochemical workstation (Chenhua Corp. Shanghai, China). A conventional three-electrode system was employed through the experiments with a GCE (3 mm in diameter) as the working electrode, a platinum electrode as the counter electrode, and a saturated calomel electrode as the reference electrode. The pH value was determined with a pHS-3C acidity meter. The morphology and element characterization was performed using a scanning electron microscope (SEM) (JSM-6700F, 15.0 kV) equipped with an energy dispersive X-ray spectrometer (EDS), respectively. A transmission electron microscope (TEM) (JEOL JEM-200CX working at 160 kV) was adopted to further probe the submicroscopic structure of the NGR-NCNTs nanocomposite.

2.2 Preparation of modified electrodes

Prior to modification, a bare GCE of 3 mm diameter was firstly polished on the chamois leather with alumina slurries until a mirror-like surface was acquired. Then the GCE was ultrasonicated in HNO_3 solution (1:1), ethanol and DDW orderly for 5 min. The ENGR-NCNT was gained by applying a potentiostatic potential of +1.7 V in 0.1 M KCl containing 200 μL 1 mg/mL NGR-NCNT/DDW. For comparison, GCE modified with electrodeposited NGR and NCNTs, namely ENGR/GCE and ENCNTs/GCE, were also prepared following the same procedure. Eventually, the as-prepared electrodes were rinsed carefully with DDW for further use.

2.3 Determination of AC and PCT in formulation tablets

The developed sensor was employed for the real sample determination. Cookie, chocolate and mike tea were chosen as the real samples. Certain amount of cookie and chocolate were ground and dissolved in ethanol. Milk tea samples were directly dissolved in ethanol. Then the centrifugal and extracted supernate were used for direct determination.

3. Results and discussion

3.1 TEM and SEM images of ENG-NCNTs nanocomposite

Before the electrode modification, morphological characterization of NGR-NCNTs nanocomposite was carried out by SEM and TEM, which was shown in Fig. 1. From the SEM image in Fig. 1(A) we can find that the NGR displays a corrugate sheet-like morphology with the nanotubes dispersed on the sheets. It is highly expected that the intrinsic high surface area of NGR as well as the unique conductivity and catalytic property of NCNTs will boost the electrochemical performance of GCE. Besides, it is found in the TEM image in Fig. 1(B) that the NCNTs spread evenly on the transparent and crimple NGR sheets without entanglement of nanotubes or re-stacking of the NGR sheets. Moreover, the NCNTs show a uniform diameter of about 10 nm, which corresponds to the original report [46]. This consistency also demonstrates the stability and reproducibility of this N-doped nanocomposite.

Additionally, to further confirm the N-doping result, EDS has been adopted to analyze the element in the NGR-NCNTs composite, which is shown in Fig. S1. It is clearly displayed that the N atom has been successfully doped into the composite.

3.2 Electrochemical behavior of CAF and VAN at ENGR-NCNTs/GCE

The electrochemical behavior of CAF and VAN at ENGR-NCNTs/GCE was qualitatively studied by CV. For comparison, bare GCE, ENCNTs/GCE and ENGR/GCE were also prepared here to electrocatalyze CAF and VAN in the same condition. Fig. 2(A) illustrates the CV responses of CAF and VAN at bare GCE (a, black), ENCNTs/GCE (b, green), ENGR/GCE (c, blue) and ENGR-NCNTs/GCE (d, red), which was carried out in 10 mL H_2SO_4 containing 10 μM VAN and 50 μM CAF. As illustrated, the poor electro-activity of CAF and VAN led to weak and unconspicuous current peaks at bare GCE. By contrast, the modified GCEs increased the electrochemical signals of both CAF and VAN in different degrees. Notably, ENGR-NCNTs/GCE exhibited the largest current responses with the most negatively shifted potential with respect to bare GCE (42 mV for CAF and 12 mV for VAN). As a result, it is indicated that the nanocomposite of NGR-NCNTs possesses the most distinguished electrocatalytic capacity towards CAF and VAN.

3.3 Optimization of preparation condition

3.3.1 The influence of buffer solution pH

In general, the oxidation process of organic molecules mainly depends on the pH of the buffer solution. Thus exploring the influence of pH on the oxidation of CAF and VAN is a necessity. SWV was chosen as the electroanalytical tool to monitor the current changes as the pH of 0.01 M H_2SO_4 buffer solution increased from 1.7 to 6, and the result was revealed in Fig. S2. The current signal of 50 μM CAF (a) and 10 μM

VAN (b) at ENGR-NCNTs/GCE decreased with the pH growth. On the contrary, their peak potential separation rose from 518 mV at pH 1.7 to 728 mV at pH 6. Although the uplifted trend of peak separation favors simultaneous determination of CAF and VAN, the prominent boost to current responses is more beneficial to the sensitivity of electrochemical sensor. As a result, pH 1.7 of 0.01 M H_2SO_4 was designated as the optimal condition for simultaneous determination of CAF and VAN.

3.3.2 The optimization of electrodeposition condition

As the NGR-NCNTs nanocomposite was modified onto the GCE through electrodeposition method, an optimization procedure on the electrodeposited potential was implemented. Specifically, CAF has been chosen individually as the measurable index due to a more distinct improvement on the oxidation response of CAF at ENGR-NCNTs/GCE. The peak current and potential changes of CAF have been recorded with the electrodeposition potential rising from 1.6 V to 2.1 V in Fig. S3(A). It can be found that the current of CAF peaked at 1.7 V and then rose again after 1.9 V. On the other hand, the peak potential of CAF in Fig. S3(B) kept growing in the ranges of 1.6 – 1.7 V and 1.8 – 2.0 V with 1.7 V and 2.0 V as the turning points, respectively. It is well known that the very positive oxidation potential may overlap with electrochemical reactions which can limit potential window from the anodic side, and thus gives rise to low reproducible analysis. [42] Considering the overall effect of electrodeposition potential on both peak current and potential, 1.7 V has been chosen as the optimal electrodeposited condition.

3.3.3 The effect of scan rate

CV technique was employed to probe into the effect of scan rate on the electrocatalysis of CAF and VAN. Fig. 3 reveals the relationships between scan rate ($v^{1/2}$) and current responses (I) as well as oxidation potentials (E_p) of 50 μM CAF (A) and 10 μM VAN (B) at the ENGR-NCNTs/GCE in 0.01 M H_2SO_4 (pH 1.7), respectively. The corresponding linear relationships between the square root of scan rate ($v^{1/2}$) *vs.* I and the logarithm of scan rate (log *v*) *vs.* E_p are illustrated in Fig. S4 (CAF) and Fig. S5 (VAN). It can be concluded from Fig. S4 that $v^{1/2}$ is proportional to I_{CAF} in the rate range of 30~190mV/s with eq.1 depicting their relationship in Table 1. In the same rate range, the linear equation describing the relationship between log *v vs.* E_p of CAF is listed as eq. 3 in Table 1. Similarly, within the range of 20~280mV/s, the eq. 2 and eq. 4 in Table 1 describing the relationships of $v^{1/2}$ *vs* I_{VAN} and log *v vs.* E_p of VAN, respectively, can be gained from Fig. S5. To sum up, all the results disclose that the individual oxidation of CAF and VAN at ENGR-NCNTs/GCE are both controlled by the diffusion process.

3.4 Determination of CAF and VAN at ENGR-NCNTs/GCE

3.4.1 Individual determination of CAF and VAN

Individual detection of CAF and VAN at ENGR-NCNTs/GCE was implemented under the optimal condition to study the corresponding electrocatalytic performance. Fig. 4(A) and (B) illustrate the SWV curves of individual detection of CAF (in-CAF) and VAN (in-VAN) respectively with the CAF concentrations ranging from 0.06 to 50

μM and VAN from 0.01 to 10 μM. The linear relationships between the concentrations and current responses are given in Fig. S6(A) and (B) correspondingly. The equations are described as eq. 5 and eq. 6 in Table 1 with the detection limits of 0.02 μM for CAF and 3.3×10^{-3} μM for VAN respectively.

These catalytic performances have been subjected to compare with previous reports and Table 2 lists the comparison result. Apparently, we can infer from the table that the ENGR-NCNTs/GCE has a more sensitive response to both VAN and CAF, which further certifies the excellent electrocatalysis of the as-made ENGR-NCNTs nanocomposite.

3.4.2 Selective determination of CAF and VAN

In view of the coexistence of CAF and VAN in a large number of beverages and food, it is of vital importance to detect them with each other's existence. Herein, CAF coexisted with 10 μM VAN (co-CAF) exhibits a linear SWV response at ENGR-NCNTs/GCE in 0.01 M H_2SO_4 (pH 1.7) within the concentration range of 0.6 – 50 μM, which is shown in Fig. 5(A). The corresponding linear regression equation of eq. 7 in Table 1 was illustrated by the calibration curve in Fig. S7(A). On the other hand, the SWV current responses of VAN with 50 μM CAF coexisted (co-VAN) at the ENGR-NCNTs/GCE is illustrated in Fig. 5(B). The according calibration curve in Fig. S7(B) can be described as eq. 8 in Table 1 with the linear rang of 0.02 – 10 μM. These results demonstrate that the coexistence of VAN do not interfere with the determination

of CAF at ENGR-NCNTs/GCE, and vice versa. This lays the foundation of simultaneous determination of CAF and VAN at ENGR-NCNTs/GCE.

3.4.3 Simultaneous determination of CAF and VAN

The simultaneous determination was carried out at the ENGR-NCNTs/GCE with the concentrations of CAF and VAN increasing synchronously. As illustrated in Fig. 6(A), the SWV responses of CAF and VAN at ENGR-NCNTs/GCE in 0.01 M H_2SO_4 (pH 1.7) display two evident current peaks with their potential separation of 518 mV. The linear relationships of simultaneous determination of CAF (si-CAF) and VAN (si-VAN) are illustrated in Fig. 6(B). The linearity range of simultaneous detection is 0.4 – 20 μM for si-CAF and 0.06 – 15 μM for si-VAN with the equation depicted as eq. 9 and eq. 10 in Table 1. These good linear relationships prove that ENGR-NCNTs/GCE can be successfully used for the simultaneous detection of CAF and VAN. As a consequence, the proposed sensor can be further used to detect real samples containing both CAF and VAN.

3.5 Reproducibility study

The sensing reproducibility of the modified electrode is very essential for the continuous and reliable detection. Six repetitive and successive measurements at ENGR-NCNTs/GCE under the optimal conditions were performed to test the reproducibility. The relative standard deviations were calculated as 2.2% for CAF and 4.1% for VAN. This experiment reflects that the superior sensing activity of the

proposed sensor is highly reproducible, which also dooms the applicability of the sensor.

3.6 Interference study

The interference study is conducted with the aim of probing the selectivity and anti-interference property of ENGR-NCNTs/GCE to CAF and VAN. Generally, the tolerance limit is taken as the maximum concentration of other foreign substances that caused a relative error of ±5% during the simultaneous determination. The interference result has been listed in Table 3. As illustrated, 10 μM alanine, phenylalanine, leucine, cysteine, uric acid and epinephrine caused little disturbances to 10 μM CAF and 1 μM VAN at ENGR-NCNTs/GCE in 0.01 M H_2SO_4 (pH 1.7). Moreover, 100 μM ascorbic acid, citric acid, glucose, maltose, sucrose, $ZnSO_4$ and $Cu(NO_3)_2$ could even hardly lead to response reductions of both CAF and VAN at ENGR-NCNTs/GCE. The acquired data prove the specificity of the ENGR-NCNTs/GCE towards the oxidation of CAF and VAN.

3.8 Analysis of real example

Several beverage and food samples have been selected to determine the content of CAF and VAN in them. Chocolate cookie has been chosen as the real sample for direct determination with the result listed in Table S1. It can be found from the SWV curves that CAF and VAN both exist in the cookie samples. Then, the simultaneous determination equations (eq. 9 and eq. 10 in Table 1) have been used for the content

calculation. The *R.S.D.* values in the table indicate that the proposed sensor presents a stable and reliable electrocatalytic performance for CAF and VAN detection.

Furthermore, the standard addition method was adopted for the determination of chocolate and two kinds of milk tea. Similarly, eq. 9 and eq. 10 in Table 1 have been chosen as the linear equations for the simultaneous determination of CAF and VAN in these samples. The satisfied recoveries and *R.S.D.* jointly imply the reliability and accuracy of ENGR-NCNTs/GCE for the practical detection of CAF and VAN.

4. Conclusion

We have succeeded to fabricate an electrochemical sensor of CAF and VAN via electrodepositing NGR-NCNTs onto the GCE. As explored in our study, the prominent boost of the oxidation currents of CAF and VAN with a distinct peak potential separation were clearly observed on ENGR-NCNTs/GCE. Compared with previous reports, the obtained higher sensitivities as well as lower determination limits obtained on this sensor also convinced the catalytic superiority of ENGR-NCNTs towards CAF and VAN. Additionally, the satisfactory real sample determinations further revealed the feasibility of the proposed sensor in practical application. In sum, this work not merely provides a facile and rapid preparation strategy for carbon nanocomposite acting as electrode modifier, but also certifies the electrocatalysis of N-doped carbon materials in electroanalytical field.

Acknowledgments

This work is supported by the National Natural Science Foundation of China (No. 21271127, 61171033), the NanoFoundation of Science and Techniques Commission of Shanghai Municipality (No. 12nm0504200), Leading Academic Discipline Project of Shanghai Municipal Education Commission (J50102). We acknowledge the Instrumental Analysis & Research Centre, Shanghai University.

References

[1] Y. Shao, S. Zhang, M. H. Engelhard, G. Li, G. Shao, Y. Wang, J. Liu, I. A. Aksay and Y. Lin, Nitrogen-doped graphene and its electrochemical applications, J. Mater. Chem. 20 (2010) 7491–7496.

[2] R. I. Jafri, N. Rajalakshmi and S. Ramaprabhu, Nitrogen doped graphene nanoplatelets as catalyst support for oxygen reduction reaction in proton exchange membrane fuel cell, J. Mater. Chem. 20 (2010) 7114–7117.

[3] J. Wu, L. Xie, Y. Li, H. Wang, Y. Ouyang, J. Guo and H. Dai, Controlled chlorine plasma reaction for noninvasive graphene doping, J. Am. Chem. Soc. 133 (2011) 19668–19671.

[4] X. Li, H. Wang, J. T. Robinson, H. Sanchez, G. Diankov and H. Dai, Simultaneous nitrogen doping and reduction of graphene oxide, J. Am. Chem. Soc. 131 (2009) 15939–15944.

[5] D. Usachov, O. Vilkov, A. Grüneis, D. Haberer, A. Fedorov, V. K. Adamchuk, A. B. Preobrajenski, P. Dudin, A. Barinov, M. Oehzelt, C. Laubschat, and D. V. Vyalikh, Nitrogen-doped graphene: efficient growth, structure, and electronic properties, Nano Lett. 11 (2011) 5401–5407.

[6] X. Lepró, Y. Vega-Cantú, F. J. Rodríguez-Macías, Y. Bando, D. Golberg, M. Terrones, Production and characterization of coaxial nanotube nunctions and networks of CN_x/CNT, Nano Lett. 7 (2007) 2220–2226.

[7] Q. H. Yang, P. X. Hou, M. Unno, S. Yamauchi, R. Saito, T. Kyotani, Dual Raman features of double coaxial carbon nanotubes with N-Doped and B-Doped multiwalls, Nano Lett. 5 (2005) 2465–2469.

[8] M. Dehonor, K. Masenelli-Varlot, A. González-Montiel, C. Gauthier, J. Y. Cavaillé, H. Terrones, M. Terrones, Nanotube brushes: polystyrene grafted covalently on CN_x nanotubes by nitroxide-mediated radical polymerization, Chem. Commun. 42 (2005) 5349–5351.

[9] B. Yue, Y. W. Ma, H. S. Tao, L. S. Yu, G. Q. Jian, X. Z. Wang, X. S. Wang, Y. N. Lu, Z. Hu, CN_x nanotubes as catalyst support to immobilize platinum nanoparticles for methanol oxidation, J. Mater. Chem. 18 (2008) 1747–1750.

[10] X. R. Wang, X. L. L. Zhang, Y. K. Yoon, P. K. Weber, H. L. Wang, J. Guo, H. J. Dai, N-Doping of graphene through electrothermal reactions with ammonia, Science 324 (2009) 768–771.

[11] D. C. Wei, Y. Q. Liu, Y. Wang, H. L. Zhang, L. P. Huang, G. Yu, Synthesis of N-doped graphene by chemical vapor deposition and its electrical properties, Nano Lett. 9 (2009) 1752–1758.

[12] L. S. Panchakarla, K. S. Subrahmanyam, S. K. Saha, A. Govindaraj, H. R. Krishnamurthy, U. V. Waghmare, C. N. R. Rao, Synthesis, structure, and properties of bron- and nitrogen-doped graphene, Adv. Mater. 21 (2009) 4726–4730.

[13] M. Calandra, F. Mauri, Electron-phonon coupling and electron self-energy in electron-doped graphene: Calculation of angular-resolved photoemission spectra, Phys. Rev. B 76 (2007) 205411–205419.

[14] S. U. Lee, R.V. Belosludov, H. Mizuseki, Y. Kawazoe, Designing nanogadgetry for nanoelectronic devices with nitrogen-doped capped carbon nanotubes, Small 5 (2009) 1769–1775.

[15] J. Zhao, G. F. Chen, L. Zhu, G. X. Li, Graphene quantum dots-based platform for the fabrication of electrochemical biosensors, Electrochem. Commun. 13 (2011) 31-33.

[16] X. L. Zhu, L. Y. Sun, Y. Y. Chen, Z. H. Ye, Z. M. Shen, G. X. Li, Combination of cascade chemical reactions with graphene–DNA interaction to develop new strategy for biosensor fabrication, Biosens. Bioelectron. 47 (2013) 32–37.

[17] G. Kucinskis, G. Bajars, J. Kleperis, Graphene in lithium ion battery cathode materials: A review, J. Power Sources 240 (2013) 66-79.

[18] C. de las Casas, W. Z. Li, A review of application of carbon nanotubes for lithium ion battery anode material, J. Power Sources 208 (2012) 74–85.

[19] Y. Wang, Z. Q. Shi, Y. Huang, Y. F. Ma, C. Y. Wang, M. M. Chen, and Y. S. Chen, Supercapacitor devices based on graphene materials, J. Phys. Chem. C 113 (2009) 13103–13107.

[20] K. J. Huang, L. Wang, J. Z. Zhang, L. L. Wang, Y. P. Mo, One-step preparation of layered molybdenum disulfide/multi-walled carbon nanotube composites for enhanced performance supercapacitor, Energy 67 (2014) 234-240.

[21] B. Li, H. Cao, J. Shao and M. Qu, Enhanced anode performances of the Fe_3O_4–Carbon–rGO three dimensional composite in lithium ion batteries, Chem. Commun. 47 (2011) 10374–10376.

[22] J. C. Carrero-Sanchez, A. L. Elías, R. Mancilla, G. Arrellín, H. Terrones, J. P. Laclette, M. Terrones, Biocompatibility and toxicological studies of carbon nanotubes doped with nitrogen, Nano Lett. 6 (2006) 1609−1616.

[23] Y. Tang, B. L. Allen, D. R. Kauffman, A. Star, Electrocatalytic activity of nitrogen-doped carbon nanotube cups, J. Am. Chem. Soc. 131 (2009) 13200−13201.

[24] S. M. Zhang, H. Y. Zhang, Q. Liu and S. L. Chen, Fe–N doped carbon nanotube/graphene composite: facile synthesis and superior electrocatalytic activity, J. Mater. Chem. A 1 (2013) 3302–3308.

[25] Y. W. Ma, L. Y. Sun, W. Huang, L. R. Zhang, J. Zhao, Q. L. Fan, and W. Huang, Three-dimensional nitrogen-doped carbon nanotubes/graphene structure used as a metal-free electrocatalyst for the oxygen reduction reaction, J. Phys. Chem. C 115 (2011) 24592–24597.

[26] S. Y. Deng, G. Q. Jian, J. P. Lei, Z. Hu, H. X. Ju, A glucose biosensor based on direct electrochemistry of glucose oxidase immobilized on nitrogen-doped carbon nanotubes, Biosens. Bioelectron. 25 (2009) 373–377.

[27] R. F. Zhou, Y. Zheng, D. Hulicova-Jurcakova, S. Z. Qiao, Enhanced electrochemical catalytic activity by copper oxide grown on nitrogen-doped reduced graphene oxide, J. Mater. Chem. A, 1 (2013)13179–13185.

[28] P. Wu, Y. D. Qian, P. Du, H. Zhang, C. X. Cai, Facile synthesis of nitrogen-doped graphene for measuring the releasing process of hydrogen peroxide from living cells, J. Mater. Chem. 22 (2012) 6402–6412.

[29] Y. Wang, Y. Y. Shao, D. W. Matson, J. H. Li, Y. H. Lin, Nitrogen-doped graphene and its application in electrochemical biosensing, ACS NANO 4 (2010) 1790–1798.

[30] S. Y. Deng, Z. T. Hou, J. P. Lei, D. J. Lin, Z. Hu, F. Yan, H. X. Ju, Signal amplification by adsorption-induced catalytic reduction of dissolved oxygen on nitrogen-doped carbon nanotubes for electrochemiluminescent immunoassay, Chem. Commun. 47 (2011) 12107–12109.

[31] G. H. Yang, L. L. Li, R. K. Rana, J. J. Zhu, Assembled gold nanoparticles on nitrogen-doped graphene for ultrasensitive electrochemical detection of matrix metalloproteinase-2, Carbon 61 (2013) 357–366.

[32] J. Borowiec, R. Wang, L. H. Zhu, J. D. Zhang, Synthesis of nitrogen-doped graphene nanosheets decorated with gold nanoparticles as an improved sensor for

electrochemical determination of chloramphenicol, Electrochim. Acta 99 (2013) 138–144.

[33] Z. H. Sheng, X. Q. Zheng, J Y. Xu, W. J. Bao, F. B. Wang, X. H. Xia, Electrochemical sensor based on nitrogen doped graphene: Simultaneous determination of ascorbic acid, dopamine and uric acid, Biosens. Bioelectron. 34 (2012) 125–131.

[34] T. W. Chen, J. Y. Xu, Z. H. Sheng, K. Wang, F. B. Wang, T. M. Liang, X. H. Xia, Enhanced electrocatalytic activity of nitrogen-doped graphene for the reduction of nitro explosives, Electrochem. Commun. 16 (2012) 30–33.

[35] H. X. Fan, Y. Li, D. Wu, H. M. Ma, K. X. Mao, D. W. Fan, B. Du, H. Li, Q. Wei, Electrochemical bisphenol A sensor based on N-doped graphene sheets, Anal. Chim. Acta 711 (2012) 24–28.

[36] S. M. Li, S. Y. Yang, Y. S. Wang, C. H. Lien, H. W. Tien, S T. Hsiao, W. H. Liao, H. P. Tsai, C. L. Chang, C. C. M. Ma, C. C. Hu, Controllable synthesis of nitrogen-doped graphene and its effect on the simultaneous electrochemical determination of ascorbic acid, dopamine, and uric acid, Carbon 59 (2013) 418–429.

[37] J. M. Goran, J. L. Lyon, and K. J. Stevenson, Amperometric detection of l-Lactate using nitrogen-doped carbon nanotubes modified with lactate oxidase, Anal. Chem. 83 (2011) 8123–8129.

[38] J. M. Goran, C. A. Favela, and K. J. Stevenson, Electrochemical oxidation of dihydronicotinamide adenine dinucleotide at nitrogen-doped carbon nanotube electrodes, Anal. Chem. 85 (2013) 9135−9141.

[39] W. W. Tu, J. P. Lei, G. Q. Jian, Z. Hu, H. X. Ju, Noncovalent assembly of picket-fence porphyrins on nitrogen-doped carbon nanotubes for highly efficient catalysis and biosensing, Chem. Eur. J. 16 (2010) 4120–4126.

[40] M. A. Raj, S. A. John, Simultaneous determination of uric acid, xanthine, hypoxanthine and caffeine in human blood serum and urine samples using electrochemically reduced graphene oxide modified electrode, Anal. Chim. Acta 771 (2013) 14–20.

[41] M. Amare, S. Admassie, Polymer modified glassy carbon electrode for the electrochemical determination of caffeine in coffee, Talanta 93 (2012) 122–128.

[42] L. Svorc, P. Tomčík, J. Svítková, M. Rievaj, D. Bustin, Voltammetric determination of caffeine in beverage samples on bare boron-doped diamond electrode, Food Chem. 135 (2012) 1198–1204.

[43] M. Aklilu, M. Tessema, M. Redi-Abshiro, Indirect voltammetric determination of caffeine content in coffee using 1, 4-benzoquinone modified carbon paste electrode, Talanta 76 (2008) 742–746.

[44] J. L. Hardcastle, C. J. Paterson, R. G. Compton, Biphasic sonoelectroanalysis: Simultaneous extraction from, and determination of vanillin in food flavoring, Electroanal. 13 (2001) 899-905.

[45] D. Y. Zheng, C. G. Hu, T. Gan, X. P. Dang, S. S. Hu, Preparation and application of a novel vanillin sensor based on biosynthesis of Au–Ag alloy nanoparticles, Sensor. Actuat. B 148 (2010) 247–252.

[46] P. Chen, T. Y. Xiao, Y. H. Qian, S. S. Li, S. H. Yu, A nitrogen-doped graphene/carbon nanotube nanocomposite with synergistically enhanced electrochemical activity, Adv. Mater. 25 (2013) 3192–3196.

[47] J. Y. Sun, K. J. Huang, S. Y. Wei, Z. W. Wu, F. P. Ren, A graphene-based electrochemical sensor for sensitive determination of caffeine, Colloid. Surf. B 84 (2011) 421–426.

[48] S. Yang, R. Yang, G. Li, L. Qu, J. Li, L. Yu, Nafion/multi-wall carbon nanotubes composite film coated glassy carbon electrode for sensitive determination of caffeine, J. Electroanal. Chem. 639 (2010) 77–82.

[49] W. J. R. Santos, M. Santhiago, I. V. P. Yoshida, L. T. K. Kubota, Electrochemical sensor based on imprinted sol-gel and nanomaterial for determination of caffeine, Sensor. Actuat. B 166-167 (2012) 739–745.

[50] S. Guo, Q. Zhu, B. Yang, J. Wang, B. Ye, Determination of caffeine content in tea based on poly(safranine T) electroactive film modified electrode, Food Chem. 129 (2011) 1311–1314.

Figure Captions

Fig. 1 SEM (A) and TEM (B) images of NGR-NCNTs.

Fig. 2 CV curves of 10 μM VAN and 50μM CAF in 0.01 M H_2SO_4 at bare GCE (a, black), ENCNTs/GCE (b, green), ENGR/GCE (c, blue) and ENGR-NCNTs/GCE (d, red).

Fig. 3 (A) CV curves of 50 μM CAF at ENGR-NCNTs/GCE in 0.1 M H_2SO_4 with scan rate ranging from (a) 30, (b) 50, (c) 70, (d) 90, (e) 130, (f) 150, (g) 190 mV s^{-1}. (B) CV curves of 10 μM VAN at ENGR-NCNTs/GCE in 0.1 M H_2SO_4 with scan rate ranging from (a)10, (b) 20, (c) 40, (d) 60, (e) 80, (f) 100, (g) 120, (h) 140, (i) 160, (j) 180, (k) 200, (l) 240, (m) 260, (n) 280 mV s^{-1}.

Fig. 4 (A) SWV curves of different CAF concentrations: (a) 0.06, (b) 0.6, (c) 2, (d) 8, (e) 10, (f) 30, (g) 50 μM at ENGR-NCNTs/GCE individually in 0.01 M H_2SO_4. (B) SWV curves of different VAN concentrations: (a) 0.01, (b) 0.06, (c) 0.1, (d) 0.2, (e) 0.6, (f) 1, (g) 2, (h) 6, (i) 10 μM at ENGR-NCNTs/GCE individually in 0.01 M H_2SO_4.

Fig. 5 (A) SWV curves of CAF ranging from (a) 0.6, (b) 2, (c) 6, (d) 15, (e) 30, (f) 50 μM at ENGR-NCNTs/GCE in 0.1 M H_2SO_4 with 10 μM VAN coexisted. (B) SWV curves of VAN ranging from (a) 0.02, (b) 0.2, (c) 0.6, (d) 1, (e) 2, (f) 5, (g) 10 μM at ENGR-NCNTs/GCE in 0.1 M H_2SO_4 with 50 μM CAF coexisted.

Fig. 6 (A) SWV curves of simultaneous determination of VAN ranging from (a) 0.06, (b) 0.1, (c) 0.6, (d) 1, (e) 2, (f) 4, (g) 15 μM and CAF ranging from (h) 0.4, (i) 0.6, (j) 2, (k) 6, (l) 10, (m) 20, (n) 30 μM at ENGR-NCNTs/GCE simultaneously in 0.1 M H_2SO_4. (B) Calibration curves for the simultaneous determination of CAF (0.4 – 20 μM) and VAN (0.06 – 15 μM).

Table 1 Different calibration curves of CAF and VAN

Eq.	Linear equations of CAF	*R*	Eq.	Linear equations of VAN	*R*
1	$I/\mu A = 2.787\ (v/mV/s)^{1/2} - 7.094$	0.999	2	$I/\mu A = 1.040\ (v/mV/s)^{1/2} - 4.257$	0.998
3	$E_p/V = 0.05534\log\ (v/mV/s) + 1.257$	0.999	4	$E_p/V = 0.0415\log\ (v/mV/s) + 0.7675$	0.998
5	$I_{in}/\mu A = 0.8579 C_{in\text{-}CAF}/\mu M + 1.232$	0.998	6	$I_{in}/\mu A = 1.917 C_{in\text{-}VAN}/\mu M + 1.182$	0.998
7	$I_{co}/\mu A = 0.3739 C_{co\text{-}CAF}/\mu M + 0.7700$	0.997	8	$I_{co}/\mu A = 1.791 C_{co\text{-}VAN}/\mu M + 1.097$	0.999
9	$I_{si}/\mu A = 1.090 C_{si\text{-}CAF}/\mu M + 0.5926$	0.999	10	$I_{si}/\mu A = 1.573 C_{si\text{-}VAN}/\mu M + 1.304$	0.999

Table 2 Comparisons of the proposed ENGR-NCNTs/GCE with previous reported electrochemical methods for CAF and VAN determination

Analytes	Modified electrodes	Technique	Linear working range (μM)	Detection limit (μM)	Ref.
CAF	PAHNSA/GCE	SWV	0.06-40	0.137	[41]
	Nafion/GR/GCE	DPV	0.4-600	0.12	[47]
	Nafion/MWCNTs/GCE	DPV	0.6-400	0.23	[48]
	MIS/MWCNTs-VTMS/GCE	DPV	0.75-40	0.22	[49]
	Nafion/PST/GCE	LSV	0.3-100	0.1	[50]
	ENGR-NCNTs/GCE	SWV	0.06-50	0.02	This work
VAN	GCE	SWV	50-300	16	[39]
	CDA/Au–AgNPs/GCE	SWV	0.2-50	0.04	[40]
	ENGR-NCNTs/GCE	SWV	0.01-10	3.3×10^{-3}	This work

MWCNTs: multi-walled carbon nanotubes, PAHNSA: poly(4-amino-3-hydroxynaphthalene sulfonic acid), MIS: molecular imprinted siloxane, VTMS: Vinyltrimethoxysilane, PST: poly(safranine T), CDA: cellulose diacetate, Au–AgNPs: Au–Ag alloy nanoparticles.

Table 3 Results of interference experiments on the current intensity of CAF and VAN on ENGR-NCNTs/GCE. (n = 3)

Interferent	Concentration (μM)	Current ratio[a]		R.S.D. (%)	
		CAF	VAN	CAF	VAN
Alanine	10	98.4	99.2	3.29	0.98
Phenylalanine	10	90.2	93.9	0.44	2.61
Leucine	10	95.3	95.2	2.40	2.10
Cysteine	10	102.1	95.0	1.30	0.49
Uric acid	10	102.2	99.1	2.51	2.66
Epinephrine	10	101.8	94.8	2.75	2.92
Ascorbic acid	100	112.4	98.3	2.54	3.44
Citric acid	400	102.4	96.6	1.22	3.36
Glucose	100	111.4	106.9	0.99	1.68
Maltose	100	102.7	96.9	1.70	0.36
Sucrose	100	98.7	96.3	3.10	3.63
$ZnSO_4$	100	104.0	99.8	3.21	1.51
$Cu(NO_3)_2$	100	101.5	95.7	2.59	4.16

[a] Ratio of currents for mixtures of interferents and 10 μM CAF or 1 μM VAN compared to that for 10 μM CAF or 1 μM VAN alone.

Table 4 Determination of CAF and VAN at ENGR-NCNTs/GCE in different food and beverage products (n = 3)

NO.	Detected (μM)		Added (μM)		Found (μM)		Recovery (%)		RSD (%)	
	CAF	VAN	CAF	VAN	CAF	VAN	CAF	VAN	CAF	VAN
R1	3.018	0.8879	10.0	3.0	13.46	3.659	104.4	95.4	1.17	1.83
R2	5.728	0.7677	10.0	3.0	15.92	3.733	101.9	98.8	0.87	1.67
R3	6.651	0.9489	10.0	3.0	16.45	3.894	98.0	98.2	0.63	1.52

R1: Chocolate; R2: Milk tea 1; R3: Milk tea 2.

Fig. 1

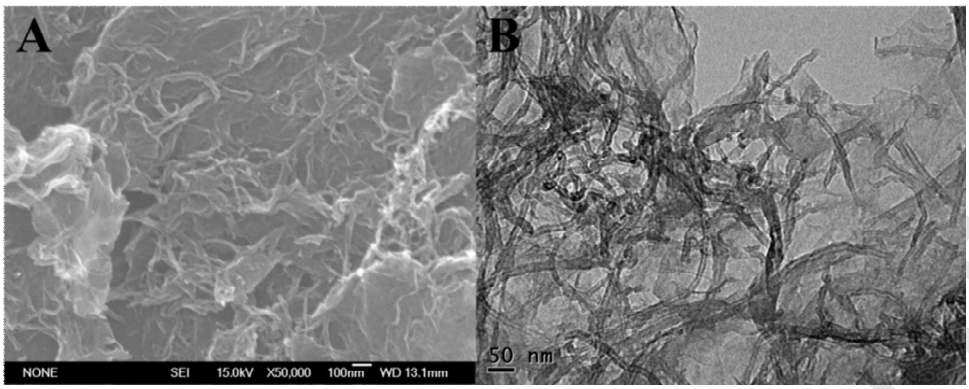

Fig. 2

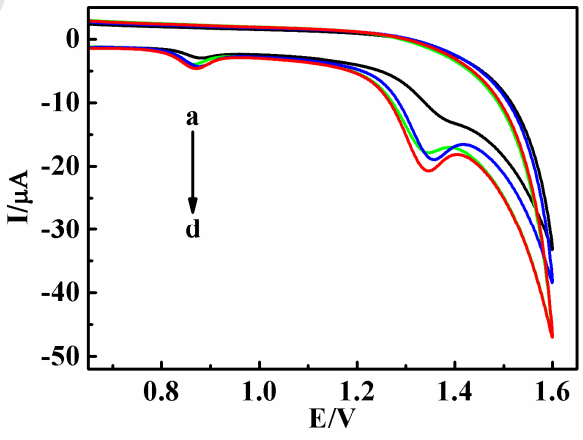

Fig. 3

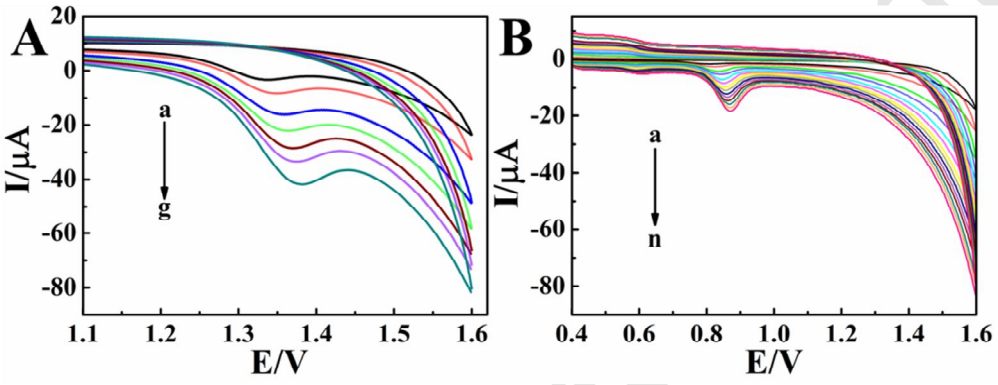

Fig. 4

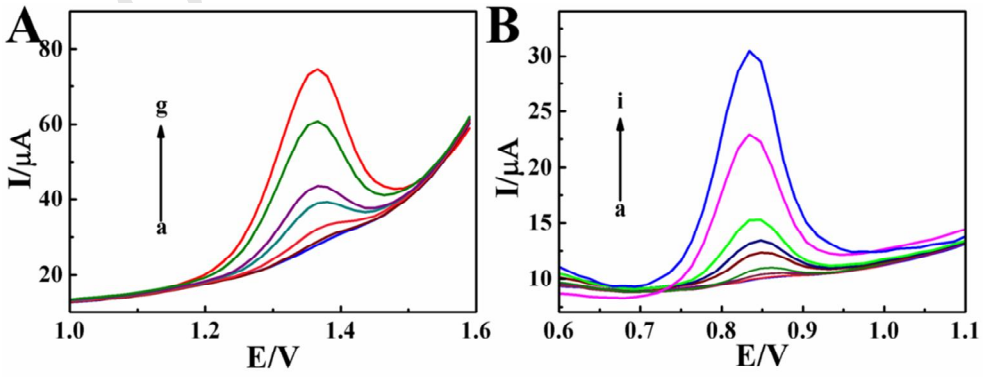

Fig. 5

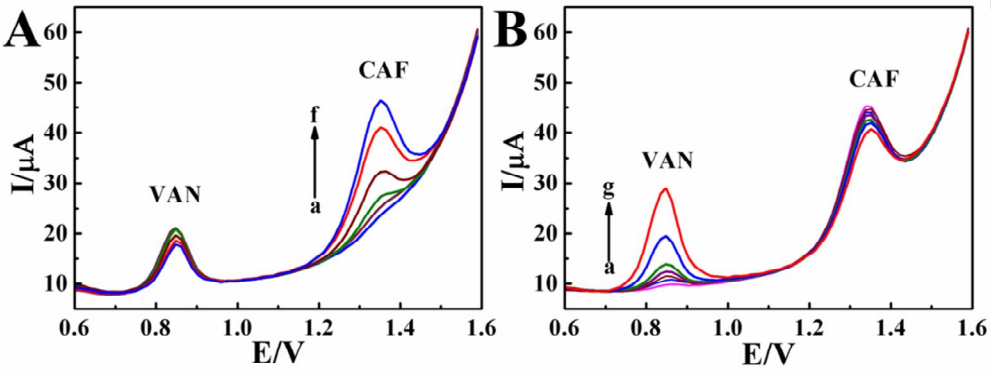

Fig. 6